Science and Innovation of Advanced Materials

The Materials Research Society of Thailand

Research Article

Engineering Hierarchically Porous Carbon Using a Facile Process: Assessment for Green Electrodes

Sopon Butcha[1,2,*], Sanchai Prayoonpokarach[2], Pongtanawat Khemthong[3]

[1] Department of Chemistry, Faculty of Science and Technology, Thammasat University (TU), Pathum Thani 12120, Thailand
[2] School of Chemistry, Institute of Science, Suranaree University of Technology (SUT), Nakhon Ratchasima 30000, Thailand
[3] National Nanotechnology Center (NANOTEC), National Science and Technology Development Agency (NSTDA), Pathum Thani 12120, Thailand

* Corresponding author e-mail: soponb22@tu.ac.th

Received: *May 17th, 2023* | ***Revised:*** *June 16th, 2023* | ***Accepted:*** *June 16th, 2023*

Abstract: Production of carbonaceous materials from waste biomass is currently gaining much attention in scientific community due to the encouragement towards a sustainable approach. However, severe pretreatment processes are still the main challenging tasks. Herein, water hyacinth (WH) is used as a precursor. Hydrothermal carbonization in acidic conditions followed by thermal activation was used for the pretreatment. A novel chemical activator CH_3COOK was employed and compared to traditional chemical activators such as $ZnCl_2$ and K_2CO_3. High surface areas and numerous micropores of synthesized carbons are found in $ZnCl_2$ activation, while carbon compounds produced from K_2CO_3 and CH_3COOK possess modest surface areas but hierarchically micro-meso-structured carbon. These findings demonstrate that the CH_3COOK could serve as both a reagent for acid-assisted hydrothermal carbonization and a doped chemical for thermal activation. The use of CH_3COOK is more ecologically and economically friendly, confirmed by reduced chemical usage and less produced wastewater. Furthermore, because the obtained carbons include a large number of nitrogen contents of around 2.0 wt%, these hierarchically porous carbons could enhance their performances as electrode materials in energy storage applications.

Keywords: Water hyacinth, Hydrothermal carbonization, Biomass conversion, Hierarchical porous carbon, Potassium acetate

1. Introduction

The growth of the world's population has caused an imbalance between the production and consumption of our feedstock, resulting in the lack of consistent access to enough food but somehow generating excessive garbage and polluting the environment [1]. Accordingly, alternative feedstock and sustainable management of the produced waste are crucial. Agricultural residues and food waste such as rice husk, corn hull, sugar cane straw, wheat straw, and coffee grinds are examples of biomass. Although there are several strategies to transform biomass into valuable products, including biodiesel, bio-coal, and alcohol, activated carbon manufacturing from these feedstocks has attracted a great deal of attention nowadays [2].

* Presented at The 4th Materials Research Society of Thailand International Conference

Activated carbons derived from a sustainable resource have several positive aspects. The resultant carbons perform remarkably well enough in electrochemical investigations due to their highly porous architectures, which feasibly enable ion or charge transport [3]. Polar functional groups on the carbon matrix, such as hydroxyl, carbonyl, carboxylate, ether, and ketone, could enhance the wettability of polar electrolytes, allowing the passage of ions/charges [3]. Additionally, since heteroatoms such as phosphorous, nitrogen, and sulfur are naturally found in the feedstock as pigment compounds or amino acids, the self-doping of heteroatoms into carbon structures is more facile and eventually provides a substitute for conventional chemical doping [4,5]. Several investigations have been achieved in doping heteroatoms into carbon structures, significantly improving electrochemical performances by introducing pseudocapacitance into the materials [5,6]. Considerably, employing heteroatom-doped carbonaceous materials as a green electrode for energy storage devices, e.g., lithium-ion batteries and supercapacitors, is thus one of the most feasible strategies in biomass utilization.

Water hyacinth (*Eichhornia crassipes*, WH) is a notorious aquatic plant with an incredible growth rate over the water surfaces, resulting in the depletion of dissolved oxygen and nutrients and negatively impacting the ecosystem [7]. On the other hand, WH is predominantly composed of cellulose, hemicellulose, and lignin, but it also has a high protein content in its composition [7]. Such renewable resources can be utilized as a precursor for producing heteroatom-doped activated carbon.

Recently, we developed an approach for producing activated carbon from spent coffee grounds using hydrothermal carbonization (HTC) in an acetic acid solution, followed by potassium hydroxide (KOH) activation [6]. The findings demonstrate the significance of acidic conditions during HTC, which would be advantageous for introducing nitrogen atoms into carbon structures [6]. However, activation of hydrochar with base reagents tends to create a higher proportion of large mesopores and produce a very low carbon yielding. On the contrary, activation with acidic chemicals such as zinc chloride ($ZnCl_2$) would enhance a larger degree of micropores in the carbon structures [8]. Although the existence of mesoporous features on carbon substrates would enhance electrolyte transport, the major of charge or ion transfer and storage is provided by the micropores [9]. Therefore, the production of carbon materials should be further optimized eventually for the hierarchical porous carbon. Rakmae and co-workers (2016) found that calcination can convert potassium acetate (CH_3COOK) to carbonate species in the zeolite pores. The CH_3COOK precursor has the benefit of promoting a great dispersion of potassium carbonate (K_2CO_3) on the zeolite support, resulting in superior catalytic performance for biodiesel production [10]. As a consequence, because CH_3COOK is an acidic medium that can be converted to basic K_2CO_3 by thermal activation, such technique is adopted for the production of biomass-based carbon materials employing HTC pretreatment in an acidic environment followed by thermal activation.

Accordingly, this contribution highlights not only a straightforward but also an effective method for utilizing WH to produce carbon materials with high surface areas and nitrogen-containing in their structure. For the WH pretreatment, HTC and thermal activation were used. $ZnCl_2$ and K_2CO_3, two typically chemical activators, were tested and compared with the novel chemical activator as potassium acetate CH_3COOK. Moreover, this study also presents preliminary results of those materials' electrochemical performances for use as green electrodes in supercapacitors. This established procedure is a potential strategy to be implemented in a practical application to facilitate activated carbon manufacturing and the SDGs in terms of converting waste into high-value goods.

2. Methodology

WH was collected from the Premprachakorn Canal in Pathum Thani, Thailand. In this study, the entire WH, including the stem, leaf, and root, was used as a sustainable resource for pretreatment. Afterward, WH was washed to eliminate dust, meshed, and dried. The WH was pretreated in an autoclave reactor using the hydrothermal method in 2 M acetic acid solution for 10 h at 180 °C. After the HTC process, WH-derived biochar was filtered, washed, and rinsed with DI water until the pH of the washing water was neutral. The biochar was then impregnated with chemical activators such as $ZnCl_2$ and K_2CO_3 in a 1:2 weight ratio of biochar : activator. Thermal activation was carried out in a tube furnace

for 2 h at 700 °C with N_2 gas flow (99.999%) at the flow rate of 350 mL·min^{-1}. The resultant carbons were collected, rinsed with a large amount of DI water until the pH reached 7.0, and dried in a vacuum oven overnight at 50 °C.

All the preceding steps were replicated when CH_3COOK was used as a chemical activator; however, the HTC was carried out in a 2 M acetic acid/potassium acetate solution (CH_3COOH/CH_3COOK). Additionally, subsequent filtering of as-prepared biochar, the biochar was subjected to thermal activation without any washing, pH adjusting, or chemical doping.

The elemental compositions of porous carbons were evaluated using an elemental analyzer (CHN62, LECO) and a sulfur analyzer for material characterization (628S, LECO). The porous architectures of the carbons were studied using N_2 adsorption-desorption analysis on an Autosorb IQ gas analyzer at -196 °C, and the materials had to be degassed for 3 h under a vacuum before analysis. The specific surface areas, pore size distribution and microporous surface area, and pore volume were calculated using the Brunauer-Emmett-Teller (BET), the Non-Localized Density Functional Theory (NLDFT) and t-plot methods, respectively. The surface morphology of carbons was examined by the scanning electron microscope (SEM) on a Hitachi SU8030. The topology of the carbon microstructure was obtained using a transmission electron microscope (TEM) on a JEOL TEM-2100. Carbon allotropes were determined using an X-ray diffractometer (XRD) on a Bruker D8 Advance with Cu Kα radiation (1.54 Å) operated at 40 kV and 40 mA, scanning in the range of 2-theta (2θ) between 10° and 80° at a rate of 0.02° min^{-1} and step time 0.5 s·degree^{-1}. Characteristics of carbons were examined using the Raman spectrometer on NT-MDT NTEGRA at the excitation wavelength (λ_{ex}) of 532 nm.

The electrochemical properties of porous carbons were investigated using a potentiostat (Metrohm Autolab) equipped with a three-electrode system, including Ag/AgCl, Pt wire, and synthesized carbons as reference, counter, and working electrodes, respectively. Working electrodes were fabricated by spluttering the slurry containing 80 activated carbons : 10 carbon black : 10 polyvinylidene fluoride (PVDF) mass ratio on the 316 stainless steel sheets with a confined area of 1 cm^{-2}. Prior to usage, the working electrodes were dried for 12 h at 60 °C in a vacuum oven. Cyclic voltammetry (CV) and galvanostatic charge/discharge (GCD) were conducted in 1 M H_2SO_4 as an electrolyte with varied scan rates and current densities. Specific capacitance (C_s) values were calculated by the following Equation 1:

$$C_s = \frac{I \cdot \Delta t}{m \cdot \Delta V} \quad (1)$$

Where I is constant discharge current (A), Δt is discharge time (s), m is mass of active materials (g), and ΔV is discharge potential range (V).

3. Results and discussion

Effect of chemical activators on physical properties of activated carbons

AC-1, AC-2, and AC-3 signify activated carbons produced through $ZnCl_2$, K_2CO_3, and CH_3COOK activation, respectively. Total utilization of the WH for the sustainable production of porous carbons was successfully investigated, demonstrating a high yield of carbon products of up to 20%. Table 1 shows the elemental compositions of carbon samples. AC-1 demonstrates carbon as a major component, but AC-2 and AC-3 show both carbon and oxygen as substantial components. The presence of oxygenated species in the carbon structure may enhance the hydrophilicity of such an activated carbon for its functions [3]. Interestingly, following the pretreatment process, the results show that nitrogen levels of almost 2.0 wt% are retained in carbon structures. Indeed, nitrogen content in the carbon structure can promote not only hydrophilicity but also pseudocapacitance for electric double-layer supercapacitors (EDLC), which can further improve electrode performance [6]. Nevertheless, non-specified elements of around 20-30% in the prepared activated carbon must be further examined.

The XRD pattern of the obtained materials (Figure 1(a)) reveals a broad peak at 2θ of about 23.0°, corresponding to amorphous graphitic carbon [11]. In contrast, sharp peaks at 2θ of 21.0° and 26.0° in the AC-1 are assigned to quartz which might be attributed to the re-crystallization of silica in the WH structure during calcination

[12]. Indeed, amorphous carbon and composite silica/carbon structures can improve the performance of energy storage devices, particularly lithium-ion batteries during the lithiation and delithiation processes [13]. Moreover, dominant peaks at 2θ of 23.0°, 29.5°, 36.0°, 39.5°, 43.1°, 47.8° and 48.7° in the AC-2 and AC-3 are interpreted as calcite presenting in ash after thermal activation [14,15]. These noticeable minerals in the XRD results are consistent with a large number of unspecified elements observed in the elemental analysis. The Raman spectra of the resultant carbons in Figure 1(b) illustrate the distinctive peaks about 1350 and 1590 cm^{-1} corresponding to the D- and G-bands of disordered and ordered carbon structures, respectively. Additionally, the D-band to G-band (I_D/I_G) ratio can be used to determine the degree of graphitization, with a lower I_D/I_G ratio indicating that the carbon materials are highly graphitized [16]. The I_D/I_G ratio of the AC-1 is 0.90, while this value increases to ~1.06 for the AC-2 and AC-3, indicating a well-developed graphitic carbon structure of the AC-1 that might enhance the electrical conductivity of activated carbons [11]. The SEM image in Figure 1(c) shows a well-developed stacked sheet structure of AC-1 with small attached carbon particles. In contrast, a very rough external surface and non-uniform carbon structure are observed in AC-2 and AC-3 (Figure 1(d-e)). The TEM image of the AC-1 in Figure 1(f) indicates dispersed worm-like micropores in the amorphous carbon matrix.

Table 1 Elemental compositions of carbon samples obtained by the CHNS analyzer

Samples	Elements (wt%)					
	C	N	O	S	H	Others
AC-1	64.27	2.51	11.03	0.33	1.51	20.35
AC-2	39.98	1.19	22.99	0.13	2.61	34.11
AC-3	37.40	1.88	25.12	0.36	2.59	32.74

Another significant property that should be considered is the textural properties since they strongly impact the transportation of ions and charge in the electrodes [17]. Figure 2(a) shows N_2 adsorption/desorption isotherms of AC-1, AC-2, and AC-3 as well as their pore size distribution histogram; in addition, the information including specific surface area (S_{BET}), microporous surface area (S_{mic}), total pore volume (V_{total}) and average pore diameter (D_{aver}) is summarized in Table 2. All samples exhibit a major characteristic of type I isotherm, revealing high N_2 uptake at low P/P_o. However, a hysteresis loop at high P/P_o can be related to type IV isotherm, demonstrating mesoporous structures. Accordingly, these results imply the formation of hierarchically porous structures of the obtained carbons. Their hierarchical porous structures can be also confirmed by the pore size distribution (Figure 2(b)), clarifying the distribution of pore diameter significantly at around 1.0 nm and partially between 2-10 nm. Interestingly, the S_{BET} of AC-1 (1353 $m^2 \cdot g^{-1}$) is around 2.6 folds higher than that of the S_{BET} of AC-2 (535 $m^2 \cdot g^{-1}$) and AC-3 (511 $m^2 \cdot g^{-1}$), while the degree of S_{mic} of 80% is prominent in AC-1 and AC-3, compared to 64% in AC-2. A higher proportion of micropores in porous carbons derived from acidic activators (AC-1 and AC-3) with respect to base activator (AC-2) can be explained by the fact that acidic activation has a low carbon content degradation rate than base activation because of the differences in the activation mode [18,19], resulting in a higher degree of micropores rather than a higher fraction of larger pores. As $ZnCl_2$ can serve as a template in the dehydration process for the formation of porosity in confined spaces inside precursor particles, the small and uniform size of the micropores is created. However, K_2CO_3 activation is typically accomplished by a redox process. The reduced metallic potassium is intercalated inside the graphitic laminar structure. Carbon is oxidized to CO or CO_2, and the solid particle degrades, resulting in a higher proportion of mesoporosity, mainly at the outermost surfaces of carbon materials [19]. The explanation is also consistent with the results of SEM images, which reveal that the external surfaces of AC-2 and AC-3 are rougher than AC-1. Therefore, the results from N_2 adsorption/desorption demonstrate beneficial aspects for the use of CH_3COOK as a chemical activator by enhancing the degradation rate of carbon contents but lowering the formation of mesoporosity. It should be noted that a large specific surface area accompanied by a predominance of micropores may promote sufficient ion or charge accumulating areas on the electrode/electrolyte interface, whereas the coexistence of larger mesopores may provide

a more facile electrolyte transport, further improving the charge/ion transference capability [17]. As a result, activated carbon with hierarchically micro/mesoporous structures is advantageous for high-performance energy storage electrodes.

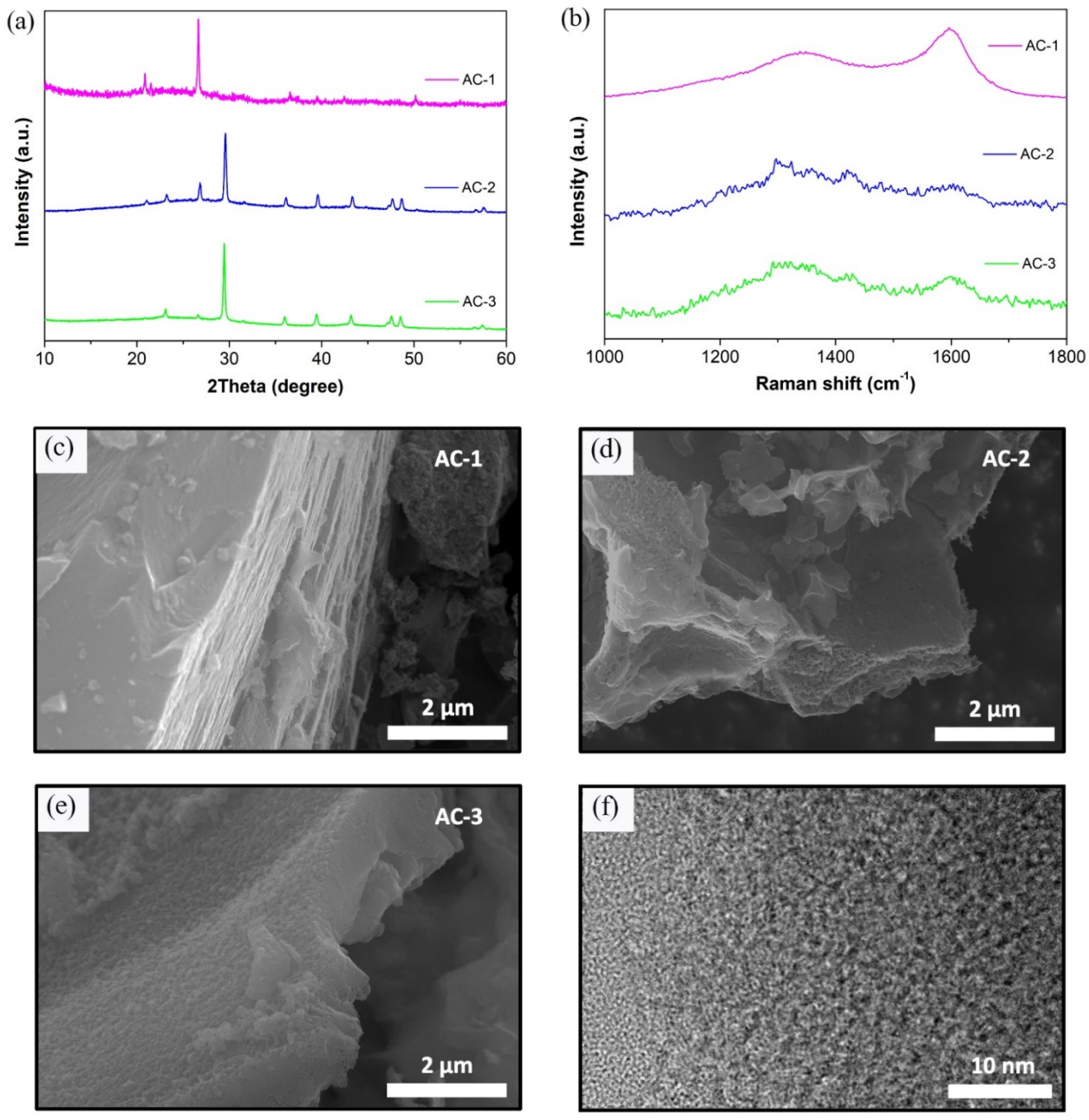

Figure 1 Characterization of carbon materials: (a) XRD patterns, (b) Raman spectra, (c), (d), (e) SEM images of the AC-1, AC-2 and AC-3, respectively, and (f) TEM image of the AC-1.

All things considered, the use of CH_3COOK as a chemical activator for WH pretreatment has several significant advantages, including no more added chemical doping during the thermal activation process, less produced wastewater during filtration and neutralization, and self-doped N contents in a hierarchically porous carbon matrix. Nevertheless, modest specific surface areas and a significant number of inorganic components in carbon frameworks, which would dramatically alter carbon's conductivity, are bottlenecks that should be further improved.

Table 2 Summarized information on textural properties of carbon samples

Samples	S_{BET}[a] ($m^2 \cdot g^{-1}$)	S_{mic}[b] ($m^2 \cdot g^{-1}$)	%S_{mic}	V_{total}[c] ($cm^3 \cdot g^{-1}$)	D_{aver}[c] (nm)
AC-1	1353	1076	79.5	0.81	1.27
AC-2	535	341	63.7	0.48	1.06
AC-3	511	409	80.0	0.36	1.06

Remarks: [a] S_{BET} was calculated from the Brunauer-Emmett-Teller (BET).

[B] S_{mic} was adopted from the Non-Localized Density Functional Theory (NLDFT).

[c] V_{total} and D_{aver} were derived from the t-plot method.

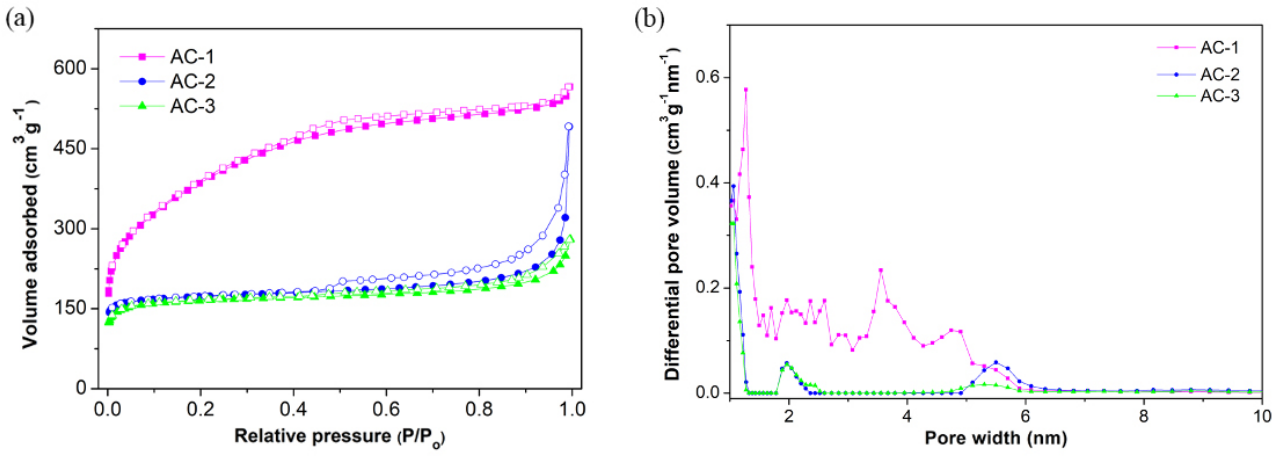

Figure 2 Textural properties of carbon samples: (a) N_2 adsorption/desorption isotherm and (b) pore size distribution histogram of AC-1 (pink), AC-2 (blue), and AC-3 (green). In cases of the N_2 adsorption/desorption isotherm, solid and space symbols represent adsorption and desorption regions, respectively.

Electrochemical performances of activated carbons

The produced activated carbons were initially used as a green electrode for a supercapacitor. All electrochemical performances were tested in a three-electrode system in 1 M H_2SO_4 as an electrolyte solution. The CV curves of all samples at a scan rate of 50 mV/s are displayed in Figure 3(a). These materials exhibit quasi-rectangular CV curves, indicating efficiently reversible supercapacitor behavior [20]. Interestingly, the larger area of the AC-1 than that of the others demonstrates its greater charge accumulating capability due to its large specific surface areas and significant N contents [21]. Consequently, AC-1 was chosen for further studies. The CV curves of the AC-1 at different scan rates shown in Figure 3(b) still maintain a distorted rectangular-like shape, implying a good EDLC paired with pseudocapacitive performance [22]. In reality, EDLC behavior results from ion or charge storage at the electrode/electrolyte interfaces, whereas pseudocapacitive performance originates from redox reactions between heteroatom moieties and ions in the electrolyte [22]. The similar shapes of CV curves at both low and high scan rates indicate that ions or charges can effectively excess into electrode surfaces [22]. Figure 3(c) shows nearly symmetric and linear GCD curves at various current densities, along with a slight distortion and a small IR drop at high current density (0.05 V at 0.5 $A \cdot g^{-1}$), confirming reversible charging/discharging and demonstrating the behavior of the EDLC coupling with pseudocapacitance reaction [22]. Furthermore, the quasi-triangle GCD curve of the AC-1 compared to the relatively symmetric GCD curve of the commercial AC demonstrates the evident pseudocapacitance of the obtained material in the H_2SO_4 electrolyte (Figure 3(d)). The specific capacitance (C_s) of electrodes at different current densities was determined and reported in Figure 3(e). The AC-1 reaches a significant C_s value of 125 $F \cdot g^{-1}$ at 1 $A \cdot g^{-1}$, while the commercial AC only possesses a value of 70 $F \cdot g^{-1}$, indicating a quite competitive capability as electrode materials for

supercapacitors. C_s values dramatically decline as the current density increases (Figure 3(e)). The decrease in C_s can be explained by insufficient path length of ions or charges in the electrolyte to transport into the electrode interfaces [23]. The cycling stability of the AC-1 was tested, as shown in Figure 3(f). The significant reduction of the C_s values can be found at approximately 50% after 500 times charge-discharge cycles at 1 $A \cdot g^{-1}$, revealing moderate capacitance retention and cycle performance. For the practical application of the synthesized material in a supercapacitor, other electrochemical tests have to be further explored such as the Electrochemical Impedance Spectroscopy (EIS), investigating in a symmetric two-electrode system or eventually symmetric coin-type supercapacitor devices.

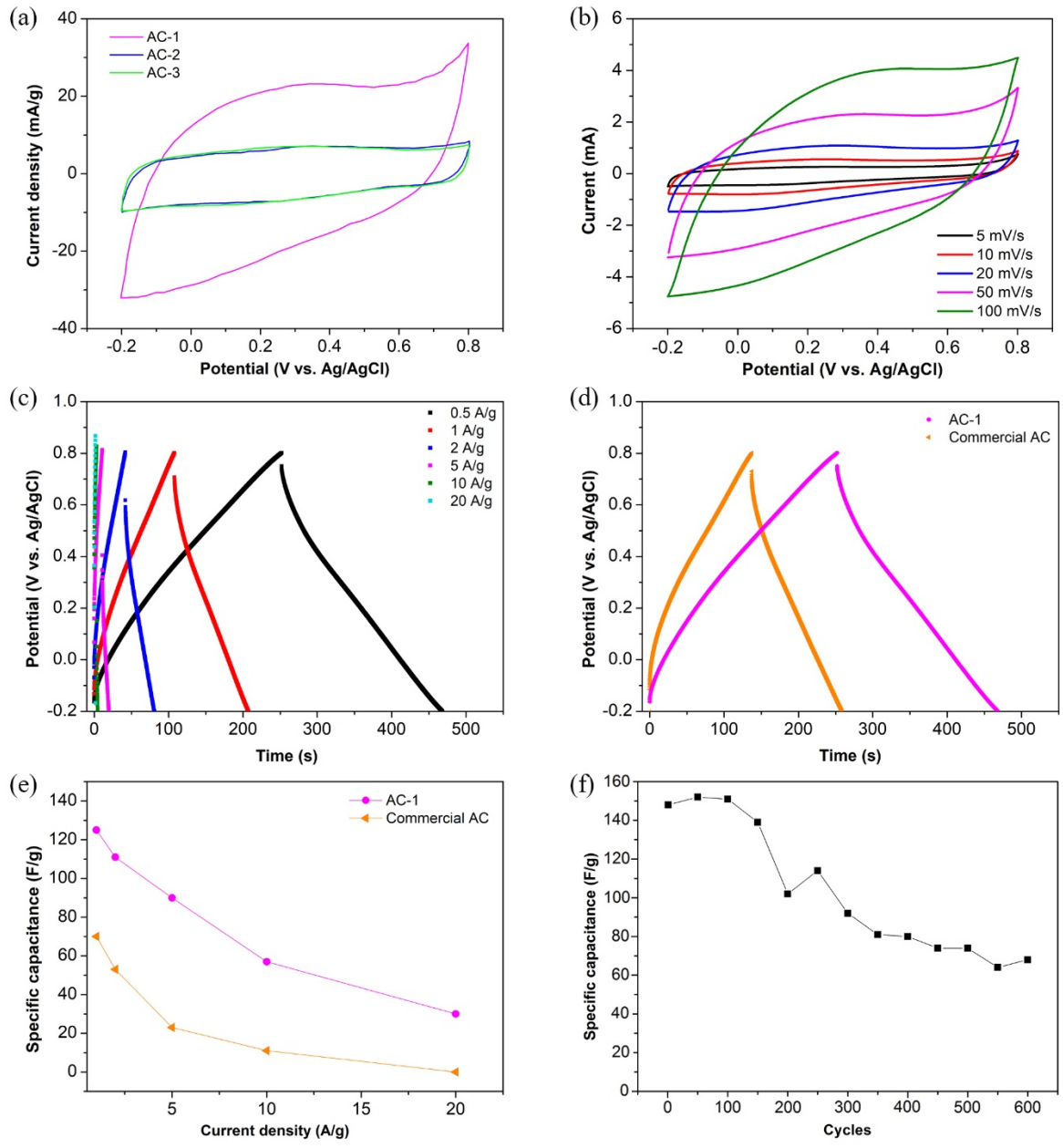

Figure 3 Electrochemical performance of activated carbons: (a) CV curves of the AC-1, AC-2, and AC-3 at a scan rate of 50 mV/s, (b) CV curves of the AC-1 at varied scan rates, (c) GCD curves of the AC-1 at different current densities, (d) GCD curves of the AC-1 compared to a commercial AC at a current density of 0.5 A/g, (e) specific capacitance versus current density of the AC-1 compared to a commercial AC, and (f) retention performance of the AC-1. Electrochemical characterization was conducted in a three-electrode system in 1 M H_2SO_4 as an electrolyte solution.

4. Conclusion

In summary, hydrothermal carbonization followed by thermal activation was applied to produce activated carbons derived from WH. A novel chemical activator CH_3COOK was applied for the pretreatment process compared to conventional $ZnCl_2$ and K_2CO_3 activators. CH_3COOK can act, at the same time, as a reagent for acid-assisted hydrothermal carbonization to enhance carbon yield and as a doped chemical for thermal activation to create porosity. Activated carbons derived from CH_3COOK possess a moderate surface area of around 500 $m^2 \cdot g^{-1}$ and show hierarchically micro/mesoporous structures. The developed pretreatment process is greener and more cost-effective than the general two-step pretreatment procedure. However, the structural, topological, and electrochemical properties of activated carbons should be closely monitored. The AC-1 has large surface areas and considerable nitrogen contents in its carbon backbone. Consequently, the AC-1 exhibits EDLC and pseudocapacitive characteristics of specific capacitance of 125 $F \cdot g^{-1}$ at 1 $A \cdot g^{-1}$, which are beneficial for energy storage devices and could be used as electrode materials for supercapacitors.

Acknowledgment

We would like to acknowledge a grant from the Department of Chemistry, Faculty of Science and Technology, TU, the Young Scientist and Technologist Program (YSTP) supported by NSTDA, and additional supports from SUT and NANOTEC.

References

[1] P. O. Ukaogo, U. Ewuzie, C. V. Onwuka, Environmental pollution: Causes, effects, and the remedies, In Microorganisms for Sustainable Environment and Health, Elsevier (2020).

[2] Y. X. Seow, Y. H. Tan, N. Mubarak, J. Kansedo, M. Khalid, M. L. Ibrahim, M. Ghasemi, A review on biochar production from different biomass wastes by recent carbonization technologies and its sustainable applications, *J. Environ. Chem. Eng.* **10** (2022) 107017.

[3] J. Wang, P. Nie, B. Ding, S. Dong, X. Hao, H. Dou, X. Zhang, Biomass derived carbon for energy storage devices, *J. Mater. Chem. A* **5** (2017) 2411-2428.

[4] Q. Abbas, R. Raza, I. Shabbir, A. Olabi, Heteroatom doped high porosity carbon nanomaterials as electrodes for energy storage in electrochemical capacitors: A review, *J. Sci.: Adv. Mater. Devices* **4** (2019) 341-352.

[5] P. Deng, S. Lei, W. Wang, W. Zhou, X. Ou, L. Chen, Y. Xiao, B. Cheng, Conversion of biomass waste to multi-heteroatom-doped carbon networks with high surface area and hierarchical porosity for advanced supercapacitors, *J. Mater. Sci.* **53** (2018) 14536-14547.

[6] T. Sangprasert, V. Sattayarut, C. Rajrujithong, P. Khanchaitit, P. Khemthong, C. Chanthad, N. Grisdanurak, Making use of the inherent nitrogen content of spent coffee grounds to create nanostructured activated carbon for supercapacitor and lithium-ion battery applications, *Diam. Relat. Mater.* **127** (2022) 109164.

[7] J. Baas-López, R. Barbosa, D. Pacheco, B. Escobar, Activated carbon from water hyacinth as electrocatalyst for oxygen reduction reaction in an alkaline fuel cell, *Int. J. Hydrog. Energy* **46** (2021) 25995-26004.

[8] R. Farma, R.I. Julita, I. Apriyani, A. Awitdrus, E. Taer, $ZnCl_2$-assisted synthesis of coffee bean bagasse-based activated carbon as a stable material for high-performance supercapacitors, *Mater. Today: Proc.* (2023). (In press: doi.org/10.1016/j.matpr.2023.01.370).

[9] X. Zhou, F. Chen, T. Bai, B. Long, Q. Liao, Y. Ren, J. Yang, Interconnected highly graphitic carbon nanosheets derived from wheat stalk as high performance anode materials for lithium ion batteries, *Green Chem.* **18** (2016) 2078-2088.

[10] S. Rakmae, C. Keawkumay, N. Osakoo, K. D. Montalbo, R. L. de Leon, P. Kidkhunthod, N. Chanlek, F. Roessner, S. Prayoonpokarach, J. Wittayakun, Realization of active species in potassium catalysts on zeolite NaY prepared by

ultrasound-assisted impregnation with acetate buffer and improved performance in transesterification of palm oil, *Fuel* **184** (2016) 512-517.

[11] Z. Zha, Z. Zhang, P. Xiang, H. Zhu, X. Shi, S. Chen, Porous graphitic carbon from mangosteen peel as efficient electrocatalyst in microbial fuel cells, *Sci. Total Environ.* **764** (2021) 142918.

[12] P. Deshmukh, J. Bhatt, D. Peshwe, S. Pathak, Determination of silica activity index and XRD, SEM and EDS studies of amorphous SiO_2 extracted from rice husk ash, *Trans. Indian Inst. Met.* **65** (2012) 63-70.

[13] Y. Liu, J. Xue, T. Zheng, J. Dahn, Mechanism of lithium insertion in hard carbons prepared by pyrolysis of epoxy resins, *Carbon* **34** (1996) 193-200.

[14] S. G. Choi, J. Chu, R. C. Brown, K. Wang, Z. Wen, Sustainable biocement production via microbially induced calcium carbonate precipitation: Use of limestone and acetic acid derived from pyrolysis of lignocellulosic biomass, *ACS Sustain. Chem. Eng.* **5** (2017) 5183-5190.

[15] M. Mäkelä, K. Yoshikawa, Ash behavior during hydrothermal treatment for solid fuel applications. Part 2: Effects of treatment conditions on industrial waste biomass, *Energy Convers. Manag.* **121** (2016) 409-414.

[16] T. Autthawong, O. Namsar, A. Yu, T. Sarakonsri, Cost-effective production of SiO_2/C and Si/C composites derived from rice husk for advanced lithium-ion battery anodes, *J. Mater. Sci. Mater. Electron.* **31** (2020) 9126-9132.

[17] L. Wei, G. Yushin, Nanostructured activated carbons from natural precursors for electrical double layer capacitors, *Nano Energy* **1** (2012) 552-565.

[18] M. Kılıç, E. Apaydın-Varol, A. E. Pütün, Preparation and surface characterization of activated carbons from Euphorbia rigida by chemical activation with $ZnCl_2$, K_2CO_3, NaOH and H_3PO_4, *Appl. Surf. Sci.* **261** (2012) 247-254.

[19] M. Molina-Sabio, F. Rodrıguez-Reinoso, Role of chemical activation in the development of carbon porosity, *Colloids. Surf.* **241** (2004) 15-25.

[20] J. S. M. Lee, M. E. Briggs, C. C. Hu, A. I. Cooper, Controlling electric double-layer capacitance and pseudocapacitance in heteroatom-doped carbons derived from hypercrosslinked microporous polymers, *Nano Energy* **46** (2018) 277-289.

[21] Y. Li, D. Zhang, Y. Zhang, J. He, Y. Wang, K. Wang, Y. Xu, H. Li, Y. Wang, Biomass-derived microporous carbon with large micropore size for high-performance supercapacitors, *J. Power Sources* **448** (2020) 227396.

[22] S. Senthilkumar, R. K. Selvan, Y. Lee, J. Melo, Electric double layer capacitor and its improved specific capacitance using redox additive electrolyte, *J. Mater. Chem. A* **1** (2013) 1086-1095.

[23] J. Li, G. Zan, Q. Wu, Nitrogen and sulfur self-doped porous carbon from brussel sprouts as electrode materials for high stable supercapacitors, *RSC Adv.* **6** (2016) 57464-57472.